European Journal of Medicinal Chemistry Reports 12 (2024) 100240

Contents lists available at ScienceDirect

European Journal of Medicinal Chemistry Reports

journal homepage: www.editorialmanager.com/ejmcr/default.aspx

Novel synthesized seleno-glycoconjugates as cosmeceutical ingredients: Antioxidant activity and in vitro skin permeation

Giovanna Cimmino [a,b], Mauro De Nisco [c], Cristina Alonso [d], Claudia Gravina [a], Vincenzo Piscopo [a], Reinier Lemos [b,e], Luisa Coderch [d], Simona Piccolella [a,*], Severina Pacifico [a], Silvana Pedatella [b]

[a] Department of Environmental, Biological and Pharmaceutical Sciences and Technologies, University of Campania "Luigi Vanvitelli", Via Vivaldi 43, 81100, Caserta, Italy
[b] Department of Chemical Sciences, University of Napoli Federico II, Via Cinthia 4, I-80126, Napoli, Italy
[c] Department of Sciences, University of Basilicata, Via dell'Ateneo Lucano 10, I-85100, Potenza, Italy
[d] Surfactants and Nanobiotechnology Department, Institute of Advanced Chemical of Catalonia of CSIC, (IQAC-CSIC), Jordi Girona 18-26, 08034, Barcelona, Spain
[e] Laboratorio de Síntesis Orgánica, Facultad de Química, Universidad de la Habana, 10400, La Habana, Cuba

ARTICLE INFO

Keywords:
Seleno-glycoconjugates
Pummerer-like rearrangement
UHPLC–HRMS
Antioxidant activity
Percutaneous absorption

ABSTRACT

Following recent successful results in the search for innovative semi-synthetic cosmeceutical Se-glycoconjugates, the work reported herein explores the development and evaluation of second-generation selenosugar-linked hydroxycinnamic acids as new potential cosmeceutical ingredients. Utilizing a Pummerer-like rearrangement for C1-acetylation, these novel compounds were synthesized and characterized using NMR spectroscopy and HRMS, confirming their structures and purity. The biological evaluation focused on their radical scavenging preliminary screening, and cytotoxic and antioxidant activities in human immortalized keratinocytes, revealing significant potential for use in skin care formulations aimed at counteracting oxidative stress and promoting skin health. Cellular uptake studies conducted on HaCaT keratinocytes using UHPLC-QqTOF-MS metabolomics demonstrated effective internalization of these compounds, which is crucial for their efficacy as topical agents. Furthermore, percutaneous absorption tests using the Franz diffusion cell method and subsequent HPLC-DAD analysis provided insights into the compound skin permeation capabilities, a critical factor for their practical application in cosmeceuticals.

1. Introduction

Cosmeceutical products have been formulated to counteract free radicals and their related skin harms achieving antioxidant, anti-inflammatory, anti-aging and photoprotective activity to provide pharmacological advantages [1]. Historically, natural compounds from plant sources, particularly polyphenols, have been the mainstay of medicine [2]. Over the years, studies on natural products as innovative cosmeceuticals have gained increasing interest, primarily due to their versatility and cost-effectiveness, which positively impact human skin health and disease [3]. Notably, advances in drug discovery have driven the cosmeceutical sector to a remarkable economic boom leading to a value of United States 68.67 billion dollars (USD) in 2024, with continued projected growth [4]. This unprecedented growth can be attributed to dermatological needs, mainly the high prevalence of skin disorders, the growing aging population, and increasing awareness about dermatological solutions such as cleaning, soothing, self-tanning, anti-acne, emollient, and antioxidant agents [5]. Recently, people have dedicated more attention to self-care, premature aging, and beauty preservation. Indeed, this aging escape not only affects baby boomers (>57 years) and X generation (>41 years) but is even exacerbated in Millennials (>26 years) and Z Generation (>16 years) [6]. This widespread interest in cosmeceuticals has motivated the search for new molecules to develop innovative and efficient products that satisfy the growing consumer demand for enhanced skin care solutions.

Despite the long-standing existence of the "cosmeceutical" concept, introduced more than 40 years ago, it is still not included in any of the guidelines published by the European Union (EU) and Food and Drug Administration (FDA) [7]. While pharmaceuticals must undergo rigorous testing for safety and efficacy, cosmeceuticals do not, which

* Corresponding author.
E-mail address: simona.piccolella@unicampania.it (S. Piccolella).

https://doi.org/10.1016/j.ejmcr.2024.100240
Received 30 September 2024; Received in revised form 6 November 2024; Accepted 7 November 2024
Available online 12 November 2024

makes the development of safe and effective products crucial [8]. Unlike drugs, cosmeceuticals have lower concentrations of active ingredients to provide cosmetic effects without requiring marketing authorization [9]. Therefore, the differentiation of cosmeceuticals from pharmaceuticals is crucial in modern dermatological practice. Pharmaceuticals are designed to alter or protect the skin from abnormal conditions, while cosmeceuticals enhance, improve, and nourish the health and beauty of the skin [10]. The use of bioactive natural products has enormously increased to address the growing market demands. Indeed, these products found large usage in protection against skin aging, environmental health-related risks, and infection. In this context, antioxidants are particularly utilized to counteract oxidative stress [11,12]. All these benefits are due to their regulatory effect on key physiological processes like metabolism, differentiation, growth, transcriptional and translational programs, as well as other life processes [13]. Despite the popularity of natural ingredients as safe products, they may hide undesirable effects such as irritant and allergic contact dermatitis, phototoxic dermatitis, and others [14]. Hence, more attention should be paid to the research and development of cosmeceuticals, proving their effectiveness, stability, and safety that require precise sources, structures, and mechanisms of skin interactions [15]. Concurrently, advances in pharmacology have identified several novel natural products, changing the therapeutic panorama, and emphasizing the importance of natural sources [16]. In fact, almost one-third of all new chemical entities, approved by the FDA, were classified as natural products or derivatives [17]. Synthetic cosmeceutical moieties can be created from scratch through chemical reactions or by chemical modification of existing natural molecules [18]. This nature-technology link offers an opportunity to develop novel active molecules in the cosmeceutical field of application.

Our research group has recently reported promising results harnessing selenosugar-linked p-coumaric, caffeic, and ferulic acid, especially in radical scavenging, wound healing properties, and cell uptake [19]. Following this path, the present work aims to go further into this investigation, focusing on a second generation (SG) of Se-sugars, obtained through the Pummerer-like rearrangement leading to C1-acetylation, conjugated to the same hydroxycinnamic acids. The structure/activity correlation of these semi-synthetic compounds has been investigated by evaluating their radical scavenging, cytotoxic, and in cell antioxidant activity. Additionally, HaCaT keratinocyte cellular intake was estimated using UHPLC-qQTOF-MS metabolomic tools, whereas percutaneous absorption was evaluated by the Franz cell test, followed by HPLC-DAD-based quantitative analysis.

2. Results and discussion

The search for new active ingredients, starting from natural products, often involves structural modifications to enhance the observed activity. Following the encouraging data regarding hydroxycinnamoyl Se-glycoconjugates, recently investigated as innovative cosmeceutical ingredients exerting antioxidant and wound-healing capacity [19], a second generation of compounds has been evaluated. Thus, three novel molecules were synthesized. Their chemical structures are depicted in Fig. 1, together with the first-generation (FG) ones and the employed hydroxycinnamic acids.

In particular, the FG Se-sugars were structurally modified by Pummerer-like rearrangement introducing an acetyl group at the C-1 position, aiming at enhancing the previously outlined biological properties and cellular uptake. Indeed, acetylation is closely related to the biological functionality of (poly)phenols by enhancing transport across cell monolayers and increasing some biological properties of the native molecules [20,21]. In this context, UHPLC-HRMS tools and HPLC-DAD were employed to evaluate their uptake in HaCaT human keratinocyte cell line and their porcine skin absorption profile, respectively.

2.1. Hydroxycinnamoyl SG Se-glycoconjugates: synthetic route and characterization

The synthesis of SG Se-glycoconjugates (**SG-3b**, **SG-4b**, and **SG-5b**), involved the conjugation via Mitsunobu reaction of HCAs (**3**, **4**, and **5**) with the seleno-sugar **SG-2**, bearing an acetyl group at the anomeric carbon atom. It was obtained from D-ribonolactone **1**, firstly converting this latter to compound **A** following the procedure reported by Serpico et al. [22]. Then, as detailed in Scheme 1 (please, refer to paragraph 4.1), the Pummerer-like rearrangement was employed to form an α-substituted selenide through the reaction of a selenoxide with acetic anhydride resulting in an acetylated α-carbon [23]. In this frame, *m*-chloroperbenzoic acid (*m*-CPBA) was used to oxidize the selenium atom of selenide **A** to afford the corresponding selenoxide **B**. The obtained crude mixture, without any further workup or purification step, due to its unstable nature, underwent the Pummerer-like rearrangement with acetic anhydride at 100 °C, yielding the acetylated product **C** (66 % overall yield). The *t*-butyldiphenylsilyl (TBDPS), which had been chosen as a selective protecting group at the C-5 position, was finally removed using tetrabutylammonium fluoride (TBAF) in anhydrous tetrahydrofuran (THF). Thus, **SG-2** was obtained (85 % yield). This latter constituted the second-generation donor to obtain new hydroxycinnamoyl Se-glycoconjugates via the Mitsunobu reaction, in which HCAs (**3**, **4**, and **5**) proved to be excellent substrates, giving **SG-3a**, **SG-4a**, and **SG-5a** (82–85 % yield). The isopropylidene group at C-2 and C-3 positions was finally removed under acid conditions to obtain the compounds of interest **SG-3b**, **SG-4b**, and **SG-5b** (69–80 % yield). Their structural characterization was performed by 1D and 2D-NMR (^{1}H and ^{13}C) with the complete assignment by COSY, HMBC, and HSQC NMR experiments. Indeed, the HMBC spectrum of the precursor **SG-2** evidenced the correlation of the proton at δ_H 2.10 (CH_3-CO) to the carbon at

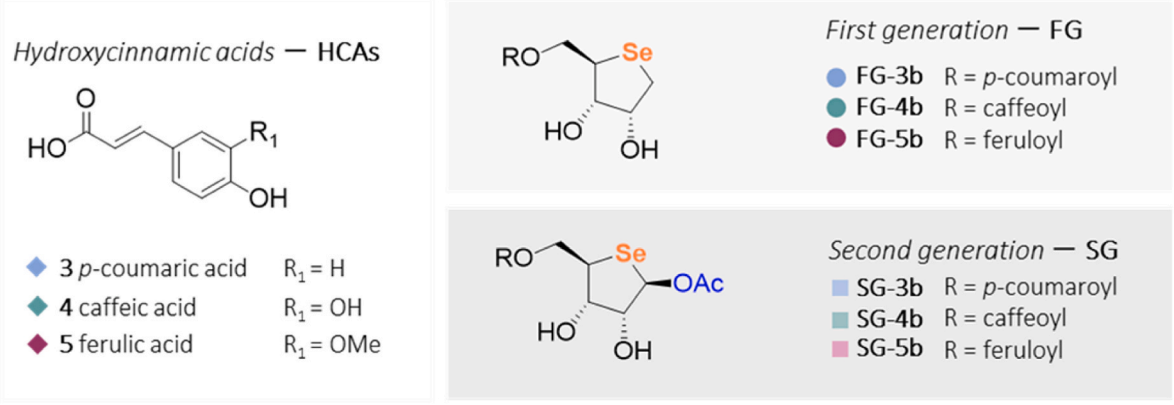

Fig. 1. Chemical structures of the first (FG) and second (SG) generation Se-glycoconjugates. The structures of hydroxycinnamic acids are also reported.

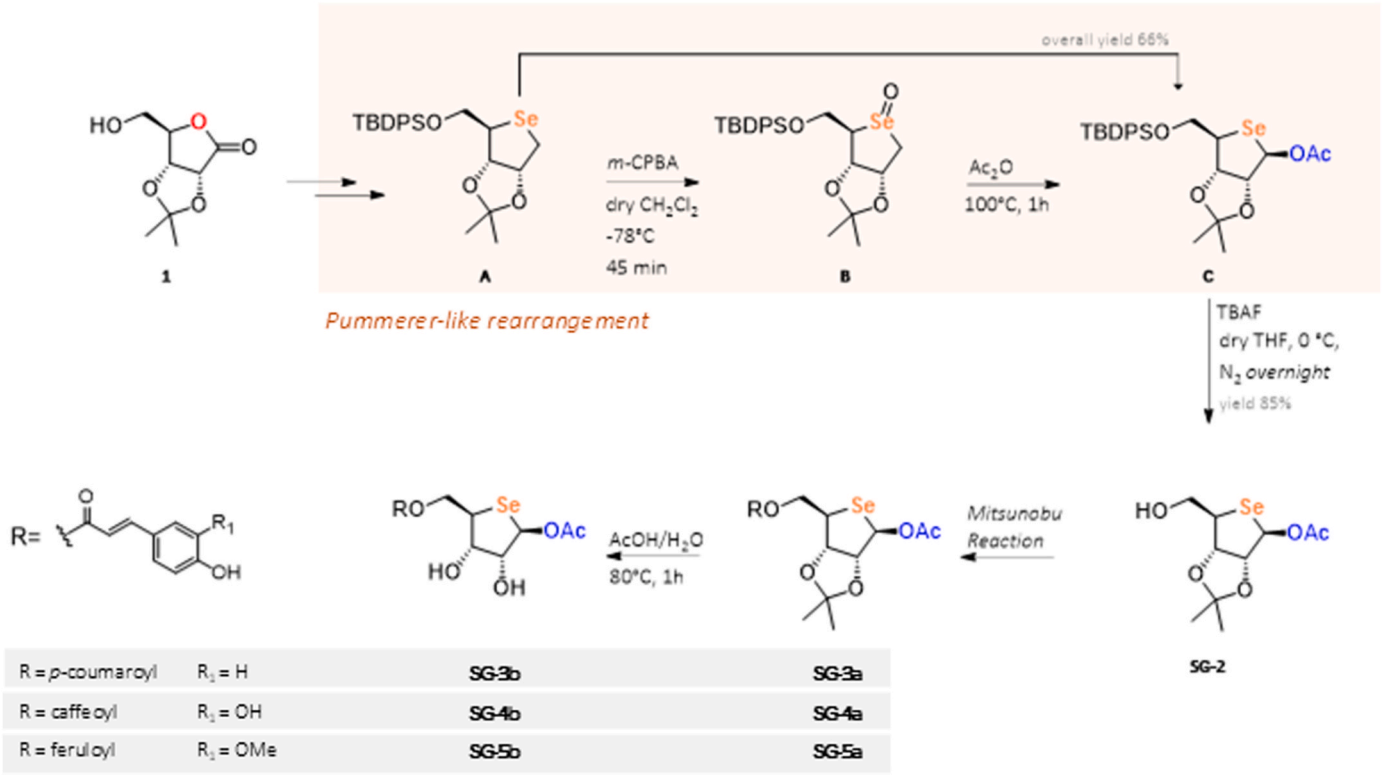

Scheme 1. Synthesis of the building block **SG-2** and SG hydroxycinnamoyl Se-glycoconjugates.

δ_C 169.3 (C-1). HSQC data supported this assignment by showing a direct correlation between the proton at δ_H 2.10 and the carbon at δ_C 21.2, due to the acetyl moiety methyl group. Instead, the COSY spectrum showed no cross-peaks for the CH_3-CO protons, confirming that they are isolated from other proton couplings. The SG Se-glycoconjugates also exhibited similar correlations, proving acetylation.

NMR findings for these latter were supported by HRMS data, which efficiently, straightforwardly, and unambiguously revealed the compound identity based on their fragmentation patterns, crucial for the metabolomic approach. TOF-MS/MS spectra of **SG-3b**, **SG-4b**, and **SG-5b** were acquired in negative ion mode and depicted in Fig. 2. They showed similar fragmentation pathways, which involved in all the cases the first neutral loss of 60.02 Da (acetic acid), attributable to the presence of the acetyl group of the Se-sugar. Thus, the fragment ions at *m/z* 340.9934, *m/z* 356.9883, and *m/z* 371.0039 were formed from deprotonated compounds **SG-3b**, **SG-4b**, and **SG-5b**, respectively. Then, the release of the sugar moiety through a charge retention fragmentation pathway [24] gave rise to the bare HCAs at *m/z* 163.0401, 179.0348, and 193.0506, which in turn fragmented as previously described [19]. Moreover, if charge migration fragmentation [24] from the HCA occurred, the fragment ions at *m/z* 212.9696 and 194.9563 were formed, attributed to the deacetylated Se-sugar and its dehydrated form.

2.2. Antiradical efficacy based on DPPH and ABTS tests

The structural features, specifically involving electron delocalization in aromatic molecules, are well known to have a strong correlation with the antiradical capacity of natural non-enzymatic antioxidants, among which phenolic compounds and their derivatives, including hydroxycinnamic ones [25]. In particular, the number, position, and type of substituents (*e.g.*, hydroxy, methoxy, and acetyl groups) can alter the charge distribution, polarity, lipophilicity, and hydrogen bonding capacity, with direct influence on the antioxidant activity [26].

Herein, DPPH and ABTS tests were carried out to have a rapid comparison among SG Se-glycoconjugates as regards the single electron and/or hydrogen atom transfer, on which the antiradical assessment is based, and also to compare the results with those previously acquired for FG compounds [19]. As depicted in Fig. 3(a), **SG-4b** showed a dose-dependent linear response in scavenging both the radical probes, reaching 83 and 86 % capacity at 50 μM tested dose. This finding is in line with the observation made for FG compounds, regardless of the difference in the esterified sugar moiety. Indeed, it has been demonstrated that also bare ferulic acid is less active than caffeic acid, whereas the esterification at the -COOH group usually does not substantially affect the activity. Instead, it is more influenced by the electron density over the aromatic ring, due to the presence of electron-donating or electron-withdrawing substituents, able to increase/decrease the bond dissociation energy involved in the antioxidant function [27].

In this case, the DPPH RSC (%) observed for **SG-4b** was slightly higher than that reported for FG Se-compounds [19], as shown by calculated IC_{50} values (Fig. 3(b)), whereas in the ABTS test the trend was the opposite. This could also be due to the two different reaction environments. Thus, it has been recommended to employ both methods, whenever feasible, to assess the antiradical capacity of the tested samples [28]. It is reasonable to assume that the chemical modification from FG to SG series compounds, *i.e.* the insertion of the acetyl group, may have been responsible for two kinds of effects. On the one hand, polarity or compound density changes could have occurred, leading to a slight improvement [29]. On the other hand, the likely enhanced steric hindrance could have reduced the accessibility of the functional groups, and, consequently, the antiradical activity towards the $ABTS^{\bullet+}$ probe [30].

2.3. Cytotoxic effects and in-cell antioxidant activity of SG Se-glycoconjugates

Cell cytotoxicity evaluation is always a mandatory step to evaluate the safety of novel molecules whatever the final application. Human immortalized keratinocytes (HaCaT) have been employed in dermatology and cosmetic research as a representative model of the epidermis

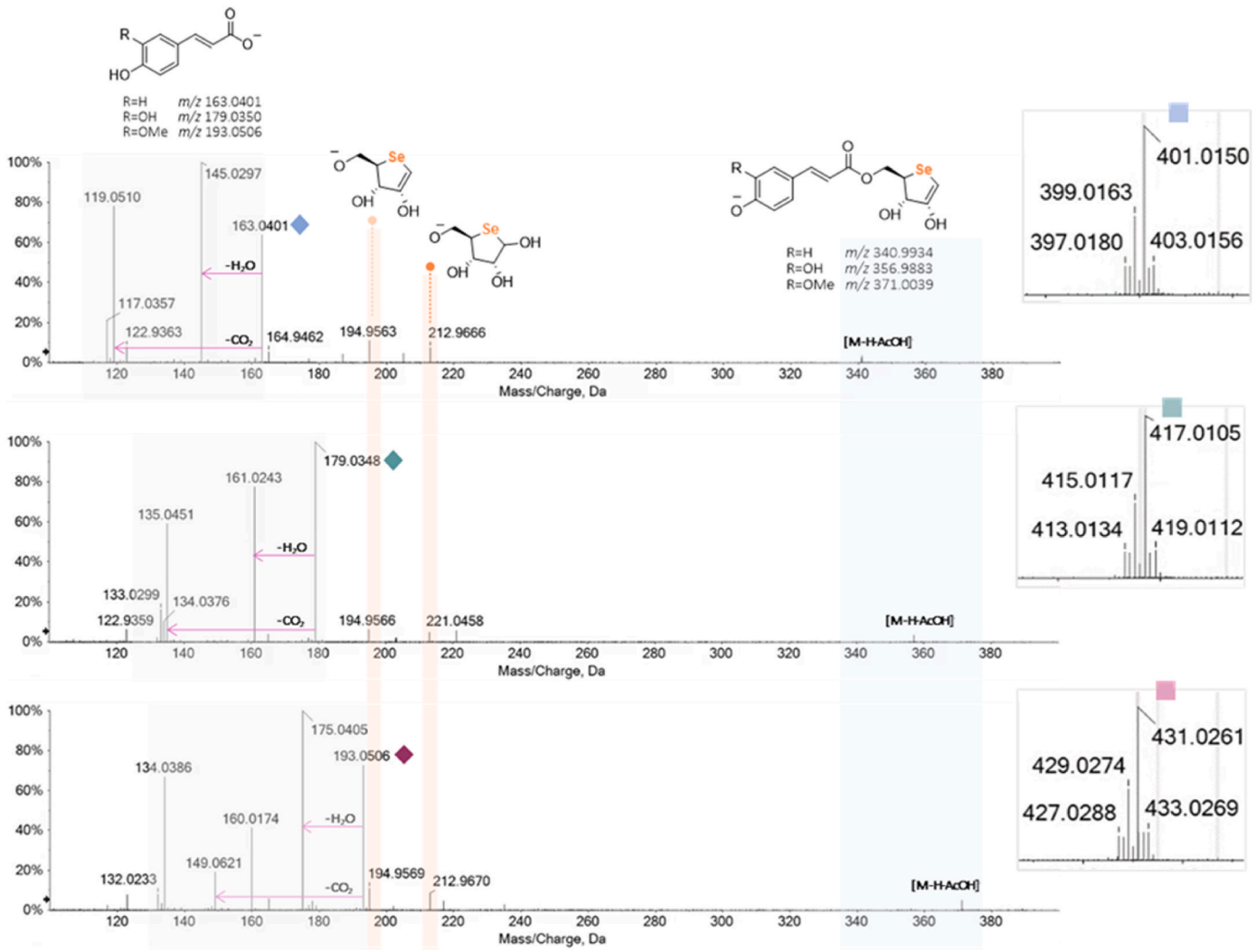

Fig. 2. TOF-MS/MS spectra for compound **SG-3b** (*m/z* 401.0150), **SG-4b** (*m/z* 417.0105) and **SG-5b** (*m/z* 431.0261). The isotopic pattern of precursor ions from TOF/MS spectra is reported in the grey boxes.

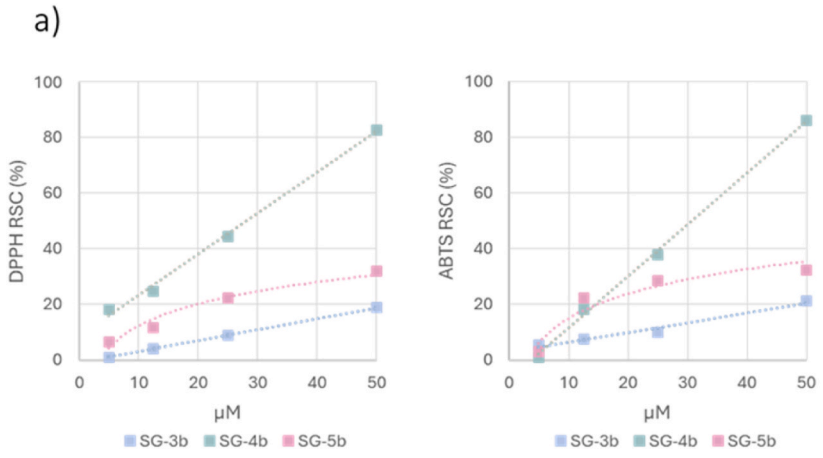

b)

	DPPH•	ABTS•+
SG-3b	> 50	> 50
FG-3b	> 50	11.3±0.7
SG-4b	30.8±1.0	28.2±1.3
FG-4b	38.9±1.9	13.2±1.1
SG-5b	> 50	> 50
FG-5b	> 50	10.5±0.7

Fig. 3. (a) Radical scavenging capacity (RSC, %) of SG Se-glycoconjugates towards DPPH and $ABTS^{+}$ radical probes, and (b) calculated IC_{50} values (μM) compared to the corresponding FG compounds. Data for these latter were from Ref. [19].

to study inflammatory and repair response, epidermal homeostasis, and the pathophysiology of skin [31]. Indeed, HaCaT cells are sensitive to oxidative insults, such as exposure to hydrogen peroxide, a known modulator of skin aging *in vivo* making them a reliable *in vitro* model [32]. Moreover, in line with our first experimental set on FG compounds [19], cytotoxicity was also assessed in SH-SY5Y S-type cells, to define the effect of the Se-sugar acetyl group on cell viability. These latter, showing an epithelial-like phenotype in their undifferentiated form, are

known to be very sensitive to oxidative stress and frequently used to evaluate the instability of the redox steady-state due to the treatment with potentially harmful agents [33].

To this purpose, both HaCaT and SH-SY5Y cell lines were treated with increasing doses (1–250 μM) of synthesized hydroxycinnamoyl derivatives **SG-3b**, **SG-4b**, and **SG-5b**. After 24h of exposure, all compounds induced a dose-dependent decrease in mitochondrial dehydrogenase activity (Fig. 4, panel a). In particular, they showed a similar trend up to 50 μM treatment dose of both cell lines, then differing in the cytotoxic effect. IC_{50} values calculated for **SG-4b** were about 2-fold

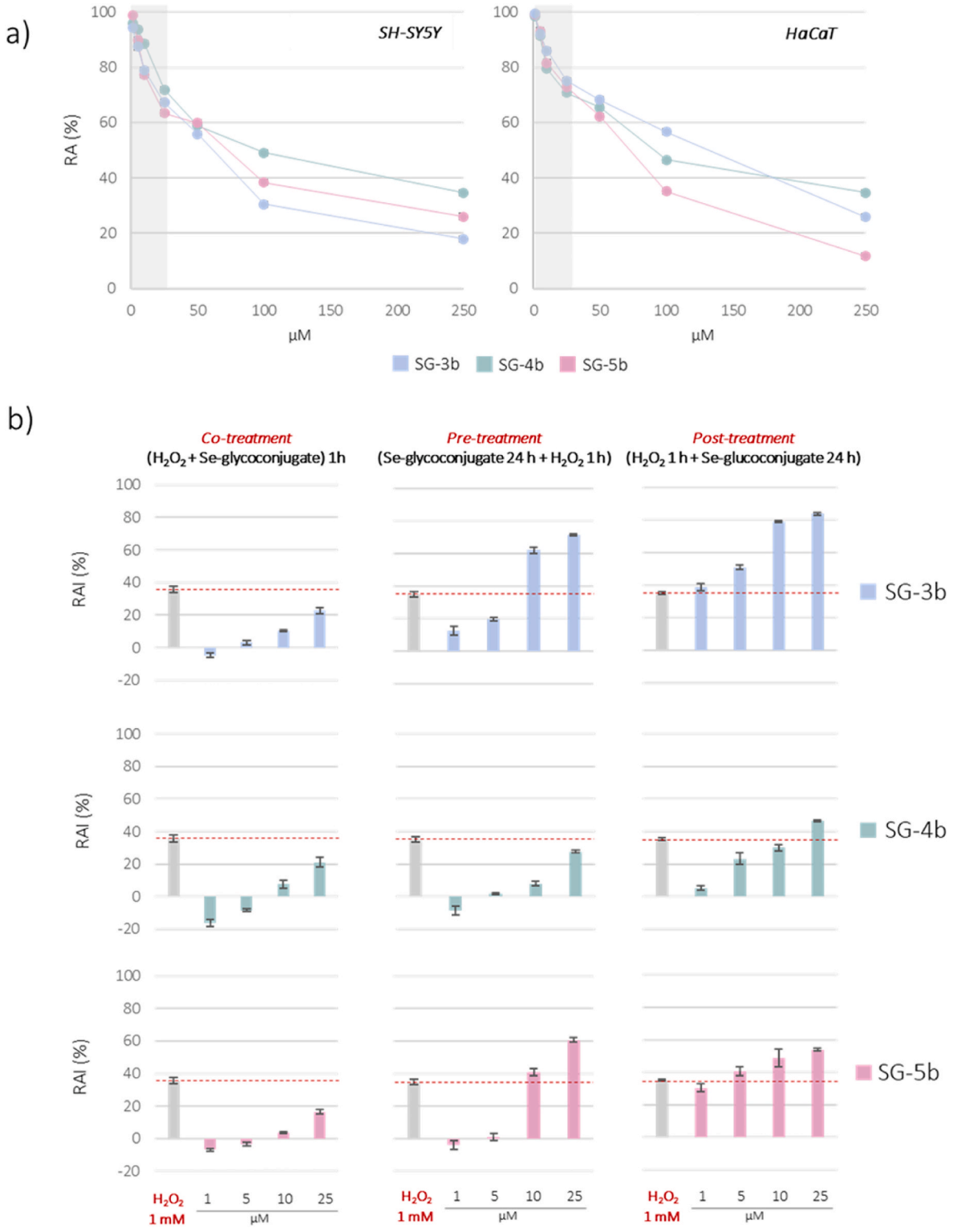

Fig. 4. (a) Redox activity (RA, %) of SG Se-glycoconjugates towards SH-SY5Y and HaCaT cell lines evaluated 24 h after treatment; (b) Redox activity inhibition (RAI, %) in HaCaT cell line *vs.* hydrogen peroxide insult evaluated in co-treatment, pre-treatment, and post-treatment with SG compounds. Red lines highlight the deviation from RAI % values ascribed to only H_2O_2-treated cells at each tested dose. (For interpretation of the references to colour in this figure legend, the reader is referred to the Web version of this article.)

higher than those of **SG-5b** in both cell models, ranging from 53 to 61 μM, and from 106 to 111 μM, in HaCaT and SH-SY5Y cells, respectively. Instead, the *p*-coumaroyl derivative (**SG-3b**) induced a different response in the redox activity, being SH-SY5Y more sensitive, as suggested by the IC_{50} equal to 46 μM, 2.6-fold lower than the value calculated for keratinocytes. These findings highlighted that the acetylated compounds showed significantly stronger inhibition of cell proliferation compared to their FG analogues, which induced only a mild influence on the redox status, even tested at the highest dose level [19]. It is reasonable to hypothesize that the increased lipophilicity due to the chemical modification can modulate the uptake and bioavailability, as well as other biological properties, facilitating the molecule cell membrane crossing and making compounds more cytotoxic [34].

Considering the exerted cytotoxicity trend, only the lower doses that did not compromise the cell redox status above 30 % (1–25 μM) were further engaged to evaluate the ability to prevent/counteract the HaCaT cell damage due to oxidative insult by hydrogen peroxide. Within this framework, in the absence of Se-glycoconjugates H_2O_2 (1 mM) was able to imbalance the mitochondrial dehydrogenase activity by 35 %, compared with untreated control cells. The experimental scheme involved three pathways: 1) a 24 h pre-treatment with SG compounds, followed by the exposure to oxidative insult with H_2O_2 (1 mM) for 1 h; 2) a post-treatment, using H_2O_2 for 1 h and then exposing the cells to SG Se-glycoconjugates for 24 h; 3) a co-treatment with simultaneous exposure of H_2O_2 and SG compounds for 1 h. As shown in Fig. 4 (panel b), the co-treatment showed a strong relevance to counteract the damage of reactive oxygen species (ROS) injuries, highlighting the ability of SG Se-glycoconjugates to effectively mitigate ROS-induced damage at all concentrations tested (1–25 μM). When the cells were pre-treated with the investigated compounds, the highest protective effect against oxidative insult was exerted by **SG-4b**, whereas *p*-coumaroyl and feruloyl derivatives at 10 and 25 μM seemed to induce an additive negative effect on redox balance. The cells appeared sensitive to **SG-3b** and **SG-5b** at the highest concentrations tested, even more in the post-treatment, suggesting a strong pro-oxidant activity that gave rise to a Redox Activity Inhibition (RAI) increase of up to 84 %.

According to the literature, HCAs are essential in preventing UV-induced skin damage, DNA oxidative stress, inflammation, and carcinogenesis on the skin [35]. These features imply their effectiveness in normal conditions, and also in skin thickness, dryness, and degradation of elastic fibres. It has been previously suggested that they can protect HaCaT cells exposed to H_2O_2, by neutralizing ROS, regenerating the antioxidant system, inhibiting the production of inflammatory cytokines, and decreasing autophagy [36]. Furthermore, HCA ability to up-regulate glutathione (GSH) content, γ-glutamate cysteine ligase (γ-GCL) mRNA, as well as catalase and glutathione peroxidase (GPx) mRNA activities and expression in irradiated HaCaT cells, has been demonstrated [37]. However, the antioxidant/pro-oxidant features in *in vitro* and *in vivo* systems may depend on several factors (*e.g.*, concentration, structure, model used, and substrate to be protected). Indeed, these compounds were reported to exert also prooxidant effects *in vitro* [38]. Among HCA derivatives, HCA amides of serotonin have been shown to protect HepG2 and HaCaT cells against oxidative stress at concentrations below 10 μM, but at higher doses, they act as pro-oxidants [39]. On the other hand, research by Zhou & Weng [40] demonstrated that butylated caffeic acid derivatives were antioxidant agents against squalene peroxidation under direct UVA exposure. The hypothesized mode of action in keratinocytes involved a decrease of peroxidized squalene-induced IL-1β secretion, a reduction of ROS generation, and a lowering of the expression of inflammatory cytokines (*e.g.*, IL-1). Additionally, Garrido et al. [41] highlighted that caffeic acid esters protect PC12 cells against hydrogen peroxide-induced oxidative damage in a dose-dependent manner. Conversely, ferulic acid esters were described as weaker antioxidants with poor protective effects. As regards the Se-sugar moiety, it has been observed that 1,4-anhydro-4-seleno-D-tallitol (SeTal) served as an antioxidant and skin tissue repairer [42], with absent clastogenic or aneugenic activity towards HepG2 or HepaRG cells [43]. Furthermore, SeTal proved to prevent endothelial dysfunction by counteracting reactive oxidants in isolated mouse aortas under acute high glucose-induced oxidative stress [44], to protect against hydrogen peroxide or hypochlorous acid-mediated oxidative damage regardless of the concentration or activities of the selenium-dependent protective enzymes TrxR and GPx [45]. Moreover, prevents the formation of 3-chlorotirosine, a typical oxidative damage biomarker, in hypochlorous acid-treated human plasma [46].

2.4. UHPLC-HRMS based metabolomics: SG compound uptake in HaCaT cells

The capability of SG compounds to cross the cell membrane for proper internalization in HaCaT cells was evaluated by UHPLC-HRMS target analysis following the same metabolomic approach previously developed [19]. The comparison of results with those acquired for FG analogues allowed us to get valuable insights into how acetylation affects compound uptake. For this purpose, the keratinocytes were treated with the 25 μM dose that ensured a minimal cytotoxic impact maintaining cellular integrity. Indeed, according to ISO 10993-5 (Biological Evaluation of Medical Devices. Part 5: Tests for in Vitro Cytotoxicity), cell viability percentages above 80 % are considered non-cytotoxic, those between 80 % and 60 % are deemed weakly cytotoxic, between 60 % and 40 % moderately cytotoxic, and below 40 % highly cytotoxic [47]. Thus, after 24 h treatment, in a preliminary cell metabolomics scenario, the extraction of the cell pellet after culture medium removal, appropriate quenching, and scraping, UHPLC-HRMS analysis was carried out. The Total Ion Current chromatograms and related TOF-MS^2 spectra confirmed that the compounds of interest were detected in the extracts from cell pellets and that structural modifications did not occur. Then, the areas under peaks from extracted ion chromatograms (XICs; Fig. 5(a)) were used for quantitation purposes, taking into account calibration curves (Fig. 5(b)) built up to this aim. The amount calculated by interpolation is reported in Fig. 5(c) as % of cell internalization, compared to FG Se-glycoconjugates.

The results underlined that acetylation significantly increased the cell membrane permeability of SG compounds, with cellular uptake exceeding 90 % for all molecules. As a result of the enhanced lipophilicity, the internalization was particularly remarkable for the ferulic acid derivative (**SG-5b**), which showed a 7.5-fold improvement, compared to its FG analogue (98 % *vs.* 13 %), followed by the *p*-coumaroyl and caffeoyl ones with a 4.4- and 3.9-fold increase, respectively. Our previous investigation on FG Se-glycoconjugates highlighted clear differences in this framework, as the compounds bearing the Se-sugars protected with the iso-propylidene group were able to cross the cell membrane more easily than those having the free Se-sugar moiety, regardless of the involved HCA [19]. Literature findings corroborate our results regarding. In fact, the effect of acetylation on bioavailability, deriving above all from a more pronounced lipophilicity, has been also demonstrated by other authors, although the compounds of interest were different from those investigated herein. In particular, Lo et al. [48] synthesized ten acyl-derivatives of the flavone luteolin, among which the 5-*O*-acetyl, proving that raising the lipophilicity induced a change in the compound bioavailability features. Specifically, Sakao et al. [21] reported that quercetin acetylation was responsible for better absorption and metabolic stability, thus ensuring boosted cancer suppression. The bioactivity and bioavailability resulted significantly improved following acetylation also for (−)-epigallocatechin-3-*O*-gallate [49]. Similarly, tangeretin chemical modification (*i.e.*, acetyl instead of methoxy group) prolonged its half-life in murine plasma and increased cellular uptake, improving cytotoxicity towards human prostate cancer cells [20].

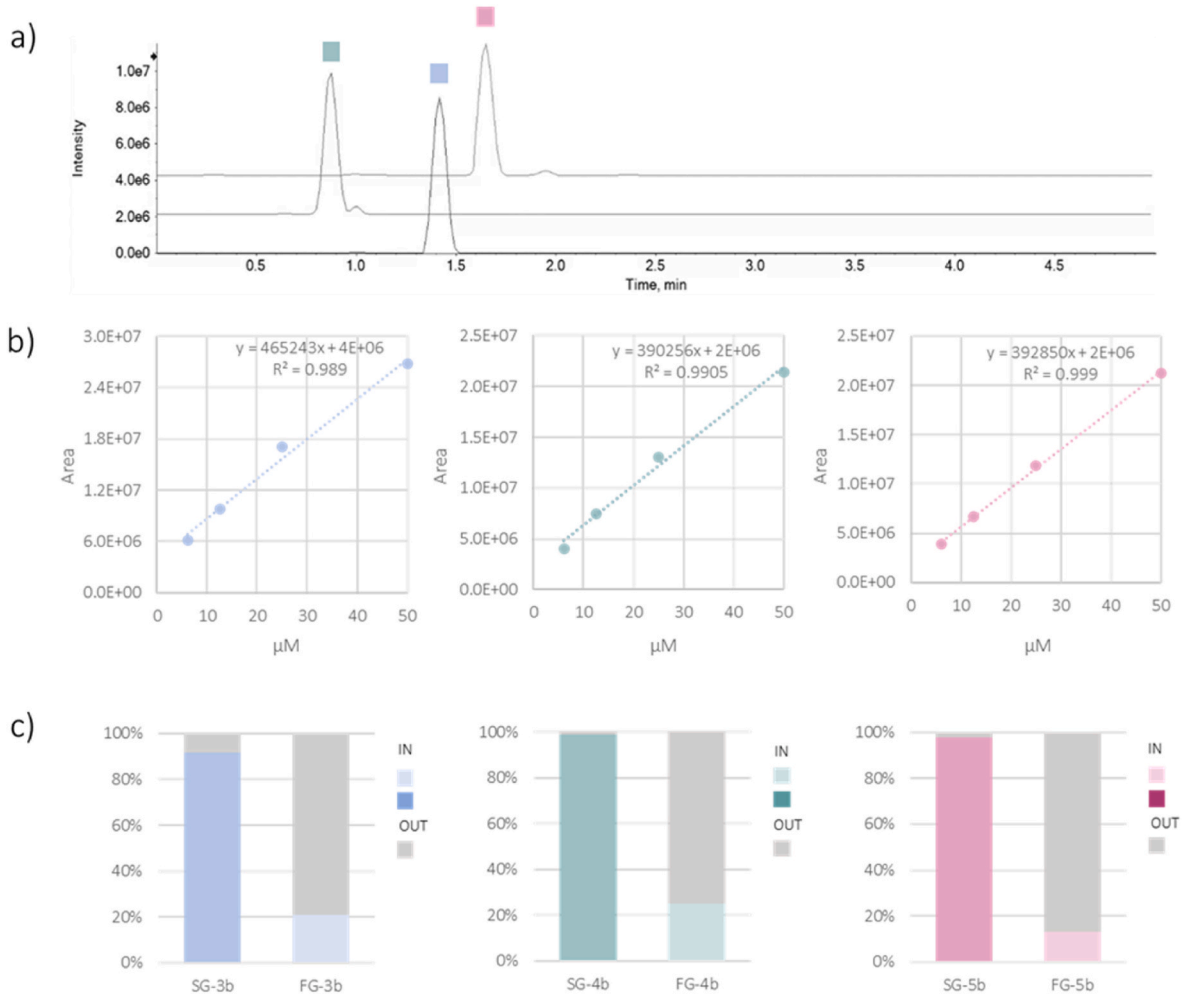

Fig. 5. (a) Extracted ion chromatograms of SG Se-glycoconjugates, and (b) their calibration curves. (c) Results from uptake evaluation in HaCaT cell pellets. Data for FG Se-glycoconjugates were reprocessed from Ref. [19].

2.5. *In vitro percutaneous absorption in HaCaT cells*

The potential of Se-glycoconjugates in percutaneous absorption within the cosmeceutical field has never been previously evaluated. The *stratum corneum* efforts as the primary mechanical barrier of the skin constrains bioactive compound penetration modulating their local or systemic effects [50]. In this pursuit, a permeation technique provides a useful strategy to assess the skin penetration profile of the compounds under study. In this framework, porcine skin has been used as a reliable model for percutaneous absorption, considering its histological and biochemical characteristics similar to human skin [51]. Hence, taking into account that the physicochemical properties of a molecule can influence the absorption, FG, SG Se-glycoconjugates, and the corresponding bare HCAs were compared after 24 h treatment to better clarify the structure-activity correlation. The obtained overall recovery (mass balance) results were acceptable (85–91 %) and the estimated Log *P* ranged from 0.76 to 1.43. The Se-glycoconjugates have more hydroxyl groups in the selenosugar moiety than bare HCAs, resulting in higher hydrophilicity corroborated by a slightly lower Log *P* value. Among tested compounds, higher concentrations of Se-glycoconjugates were detected on the skin surface (W) in comparison to bare HCAs. Fig. 6(a) depicts the distribution of the compounds under investigation, indicated as µg/cm^2, in the *stratum corneum* (SC), viable epidermis (E), dermis (D), and receptor fluid (RF) layers of the skin.

All skin compartments, except for **SG-5b** and **SG-3b**, contained the compounds when applied topically (Fig. 6(b)). HCAs showed the highest percentages of penetration (>15 %) corroborated by their highest Log *P* values. Conversely, smaller concentrations of FG Se-glycoconjugates were found in SC, E, D, and FR. A similar trend was observed in the percutaneous absorption values (3.38–5.64 %) for SG. The quantity of **FG-5b** in the inner skin layer revealed a greater penetration rate than other FG Se-derivatives. However, **SG-4b** was the only SG derivative detected in the RF compartment. Among Se-glycoconjugates, greater overall skin penetration was expected for smaller compounds, such as deacetylated derivatives (FG). Indeed, FG displayed a greater skin absorption capacity than SG in terms of global percutaneous absorption (Fig. 6(b)). Unexpectedly, the detected percutaneous absorption profile of **3b** derivative was similar for FG and SG.

Molecular weight (MW), lipophilicity, hydrogen bonding, and solubility of the molecules assume a crucial function in percutaneous absorption into the skin layer [52]. The Se-glycoconjugates had a lower lipophilicity and consequently less permeation due to sugar presence. This latter significantly affected the skin permeation behaviour, as previously reported [53]. However percutaneous absorption cannot be solely ascribed to it. Also, a higher MW than their bare HCAs affect their permeability. Indeed, in our findings, the skin penetration of SG Se-glycoconjugates was typically lower than FG. Chemical structure modification can affect the molecule hydrophobic interactions with receptors, metabolism, toxicity in biological systems, and absorption [54]. In line with this hypothesis, Chuang et al. [55] demonstrated how the flavonoid glycosides exerted a lower absorption than aglycones. Herein, acetylation was able to further decrease skin penetration [56].

a)

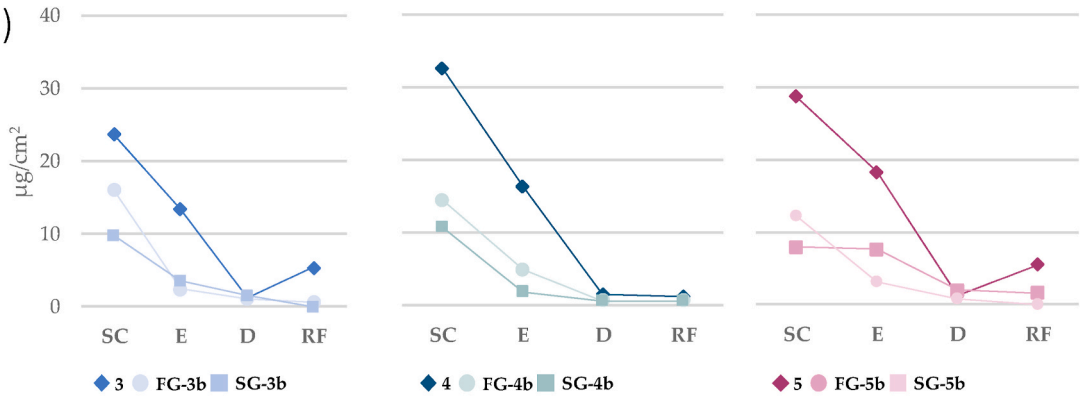

b)

	HCAs			First Generation			Second Generation		
%	3	4	5	FG-3b	FG-4b	FG-5b	SG-3b	SG-4b	SG-5b
W	55.35±9.38	55.59±11.32	51.11±11.45	74.12±2.13	80.12±3.31	70.92±9.54	81.86±3.53	82.68±2.38	81.59±2.33
SC	23.46±4.72	28.07±9.69	26.51±8.78	19.25±2.08	13.51±3.48	8.28±1.19	10.96±3.00	12.34±2.83	12.85±0.96
R	1.40±1.65	0.99±0.40	0.56±0.09	1.40±0.55	0.74±0.22	8.08±7.87	1.65±1.62	1.60±0.80	1.47±0.54
E	12.98±4.61	12.96±4.11	17.05±6.70	2.86±0.89	4.57±1.27	7.97±1.57	3.90±2.40	2.01±0.63	3.19±1.02
D	1.21±0.51	1.19±1.01	1.11±0.30	1.29±0.17	0.54±0.18	2.07±0.99	1.64±0.54	0.65±0.10	0.90±0.14
RF	5.60±7.11	1.21±1.39	3.67±2.95	1.08±0.11	0.53±0.93	2.68±0.75	B.L.D.	0.72±1.25	0.00±0.00
Perc.Abs.	19.79±3.46	15.36±3.31	21.83±4.09	5.23±0.90	5.64±1.16	12.73±2.22	5.54±1.95	3.38±1.92	4.09±0.92

Fig. 6. (a) Distribution of compounds in pig skin expressed as µg/cm^2 *per* surface of the skin layers. (b) Normalized amounts of tested compounds, expressed as % in the viable epidermis (E), dermis (D), and receptor fluid (RF) (*percutaneous absorption*), and skin surface (W), *stratum corneum* (SC), and rest of skin (R). B.L.D = Below Limit of Detection.

This approach might be used to modulate compound permeability and their putative function as antioxidants in lipid *stratum corneum* to inhibit the induction of peroxidation. In this context, the percutaneous absorption, transdermal delivery efficiency, and functional efficacy of HCAs in protecting against atmospheric pollutants and reducing the development of erythema and skin pigmentation due to UV radiation exposure have all been studied over the years [51]. The *stratum corneum* also acts as a reservoir allowing the delayed diffusion of antioxidants to the innermost layers of the skin. According to the skin healing and antioxidant properties of Se-sugars [42], Se-glycoconjugates appear to be a promising class of selenium-containing compounds poised to bring significant breakthroughs in cosmeceuticals. Indeed, SeTal enhanced skin tissue healing with topical application in a murine model [57]. This finding was further corroborated using gelatine and alginate polymeric films enriched with SeTal [58].

3. Conclusion

A new route for synthesizing seleno-glyconjugates has been developed, exploiting a Pummerer-like rearrangement and Mitsunobu reaction. The chemical structures were confirmed by NMR and UHPLC/HRMS techniques. A first evaluation of cell viability towards HaCaT and SH-SY5Y showed a dose-dependent cytotoxicity suggesting that the insertion of the acetyl group on Se-glycoconjugates could affect mitochondrial redox activity above 25 µM treatment dose. When the cells were pre-treated with low doses, the highest protective effect against oxidative insult induced by H_2O_2 was exerted by the caffeoyl derivative, whereas *p*-coumaroyl and feruloyl derivatives at 10 and 25 µM seemed to induce an additive imbalance on the redox status. Furthermore, cellular uptake of acetylated Se-glycoconjugates increased massively if compared to FG molecules, suggesting that acetylation may be used as an effective strategy to modulate their effectiveness. Additionally, the evaluation of percutaneous absorption using the Cell Franz highlighted various permeation profiles depending on different Se-glycoconjugation. This work contributes to opening new avenues for the development of Se-glycoconjugates as potential cosmeceutical agents, particularly in the field of antioxidant activity. Future research will focus on optimizing their practical application in skincare products.

4. Experimental section

4.1. Synthesis of second generation (SG) Se-glycoconjugates and structure elucidation

A new acetylated selenosugar (**SG-2**) was synthesized by the Pummerer-like rearrangement (Scheme 1). Additionally, it was employed in the Mitsunobu reaction with hydroxycinnamic acids (*p*-coumaric **3**, caffeic **4**, and ferulic acid **5**), following a defined strategy outlined by Serpico et al. [22]. Details regarding each synthetic step are provided below. The structures of the synthesized compounds were defined by NMR spectroscopy and High-Resolution Mass Spectrometry (HRMS). The ^{1}H and ^{13}C NMR spectra were recorded at 500 and 125 MHz, respectively, when a Varian Inova 500 MHz spectrometer (Varian, Palo Alto, USA) or 400 and 100 MHz, respectively, when a Bruker DRX 400 MHz spectrometer (Bruker, Milan, Italy) was utilized. $CDCl_3$ was the solvent unless differently specified. ^{1}H–^{1}H COSY experiments confirmed the proton couplings. The heteronuclear chemical shift correlations were found using Heteronuclear Multiple Quantum Coherence (HMQC) and Heteronuclear Multiple Bond Correlation (HMBC) pulse sequences. The AB SCIEX Triple TOF® 4600 mass spectrometer (AB Sciex, Concord, ON, Canada) equipped with a DuoSpray™ (ESI and APCI) ion source and a hybrid QqTOF analyzer was used for HRMS and MS/MS investigations of **SG-3b**, **SG-4b**, and **SG-5b** in negative ionization mode. The APCI probe was used for the fully automatic mass calibration by the Calibrant Delivery System (CDS) before MS and MS/MS experiments. The source parameters were curtain gas 35 psi, nebulizer and heated gases 60 psi, ion spray voltage −4.5 kV, interface heater temperature 600 °C, declustering potential (DP) −70 V and collision energy (CE) −35 ± 15 V. Analyst® TF 1.7 software (AB Sciex, Concord, ON, Canada) was used to control the instrument, whereas MS data were processed using

PeakView® 2.2 software (AB Sciex, Concord, ON, Canada).

4.2. Synthesis of O-acetyl-5-O-t-butyldiphenylsilyl-4-deoxy-2,3-O-isopropylidene-4-seleno-β-D-ribofuranoside (C)

In a 50 mL flask, *m*-chloroperbenzoic acid (*m*-CPBA; 70 %) (1.03 g, 4.20 mmol) and selenosugar **A** (1.81 g, 3.81 mmol) were dissolved in 15 mL of dry dichloromethane under argon flow at −78 °C and stirred for 45 min. The reaction mixture was washed with saturated $NaHCO_3$ solution (2 × 20 mL) and brine (20 mL). The organic phase was dried over anhydrous Na_2SO_4 and the solvent was removed under reduced pressure. The crude residue (**B**) was dissolved in acetic anhydride (16 mL, 3.82 mmol) in a flask equipped with a reflux condenser and heated at 100 °C for 1 h. The solvent was removed under reduced pressure and the obtained residue was dissolved in 15 mL of ethyl acetate. The solution was washed with water (20 mL), saturated $NaHCO_3$ solution (2 × 20 mL), and brine (20 mL). The organic phase was dried over anhydrous Na_2SO_4 and evaporated to dryness under reduced pressure. The obtained crude oil was purified by silica gel column chromatography, using petroleum ether:ethyl acetate (in increasing polarity gradient from 100:0 to 95:5) as the mobile phase to give the pure product **C** as a pale yellow-syrup (1.34 g, 2.51 mmol, 66 %). ^{1}H NMR (500 MHz, $CDCl_3$, Fig. S1): δ 7.70–7.66 (m, 4H, HAr), 7.45–7.38 (m, 6H, HAr), 6.17 (dt, $J_{H,Se}$ = 16.1 Hz, J = 0.7 Hz, 1H, H1), 5.09 (dd, J = 5.4, 0.8 Hz, 1H, H3), 4.72 (dd, J = 5.4, 0.7 Hz, 1H, H2), 3.87 (dd, J = 9.9, 5.3 Hz, 1H, H5a), 3.82 (m, 1H, H4), 3.76 (dd, J = 5.4, 0.8 Hz, 1H, H5b), 1.89 (s, 3H, CH_3-CO), 1.33 (s, 3H, CH_3), 1.12 (s, 3H, CH_3), 1.10 (s, 9H, $SiC(CH_3)_3$). ^{13}C NMR (125 MHz, $CDCl_3$, Fig. S1): δ 169.2, 135.6, 134.8, 129.9, 127.7, 110.4, 89.9, 86.2, 82.4, 66.6, 51.7, 26.9, 26.7, 24.6, 21.1, 19.3. Anal. Calcd for $C_{26}H_{34}O_5SeSi$: C, 58.52; H, 6.42. Found: C, 58.48; H, 6.44.

4.3. Synthesis of O-acetyl-2,3-O-isopropylidene-4-deoxy-4-seleno-β-D-ribofuranoside (SG-2)

A solution of TBAF (7.5 mL, 1 M in THF, 7,5 mmol) was added to the magnetically stirred solution of **C** (1.10 g, 3.74 mmol) in anhydrous THF (60 mL) at 0 °C under a nitrogen atmosphere, and the mixture was stirred at room temperature for 3h. The evaporation of the solvent under reduced pressure gave a crude residue that was purified by silica gel column chromatography using *n*-hexane:ethyl acetate (6:4) as the mobile phase to give the pure product **SG-2** as a pale yellow-syrup (0.668 g, 2.62 mmol, 85 %). ^{1}H NMR (500 MHz, $CDCl_3$, Fig. S2): δ 6.28 (bt, $J_{H,Se}$ = 16.1 Hz, 1H, H1), 4.99 (d, J = 5.4 Hz, 1H, H3), 4.95 (d, J = 5.4 Hz, 1H, H2), 3.88 (m, 1H, H4), 3.82 (dd, J = 11.6, 5.6 Hz, 1H, H5a), 3.77 (dd, J = 11.6, 6.6 Hz, 1H, H5b), 2.10 (s, 3H, CH_3-CO), 1.53 (s, 3H, CH_3), 1.33 (s, 3H, CH_3).^{13}C NMR (125 MHz, $CDCl_3$, Fig. S2): δ 169.3, 110.6, 90.6, 87.3, 82.8, 65.2, 53.6, 26.8, 24.6, 21.2. Anal. Calcd for $C_{10}H_{16}O_5Se$: C, 40.69; H, 5.46. Found: C, 40.67; H, 5.44.

4.4. Mitsunobu reaction: preparation of glycoconjugates SG-3a, SG-4a, and SG-5a

Diisopropyl azodicarboxylate (DIAD) (0.303 mL, 1.5 mmol) was added to a triphenylphosphine (TPP) (0.393 g, 1.5 mmol) solution in anhydrous THF (2.3 mL) under magnetic stirring at 0 °C under N_2. After 15 min, a solution containing **SG-2** (0.200 g, 1.0 mmol) and each hydroxycinnamic acid (1.5 mmol) in anhydrous THF (3.0 mL) was added dropwise. The reaction mixture was stirred at room temperature for three days. The solvent was evaporated under reduced pressure and replaced with EtOAc. The organic layer was washed with brine and dried (Na_2SO_4). The evaporation of the solvent under reduced pressure gave a crude residue that was purified by silica gel column chromatography (*n*-hexane:diethyl ether 7:3 (v/v)) to give the pure products **SG-3a**, **SG-4a**, and **SG-5a.**

(*E*)-*O*-acetyl-5-((3-(4-hydroxyphenyl)acryloyl)oxy)-4-deoxy-2,3-*O*-isopropylidene-4-seleno-D-ribofuranoside (SG-3a) was obtained as oil (82 %). ^{1}H NMR (500 MHz, $CDCl_3$, Fig. S3): δ 7.67 (d, J = 15.9 Hz, 1H, H8), 7.43 (d, J = 8.0 Hz, 2H, H10), 6.87 (d, J = 8.0 Hz, 2H, H11), 6.34–6.25 (m, 2H, H7, H1), 5.05 (bd, J = 5.0 Hz, 1H, H3), 5.02 (bd, J = 5.3 Hz, 1H, H2), 4.43 (dd, J = 11.6, 5.6 Hz, H5b), 4.33 (m, 1H, H5a), 3.92 (dd, J = 10.2, 5.5 Hz, 1H, H4), 2.09 (s, 3H, CH_3), 1.53 (s, 3H, CH_3), 1.34 (s, 3H, CH_3). ^{13}C NMR (125 MHz, $CDCl_3$, Fig. S3): δ 169.5, 167.1, 158.8, 145.6, 130.1, 126.5, 116.0, 114.3, 110.8, 90.2, 86.7, 82.7, 66.2, 48.4, 26.6, 24.7, 21.3. Anal. Calcd for $C_{19}H_{22}O_7Se$: C, 51.71; H, 5.02. Found: C, 51.70; H, 5.11.

(*E*)-*O*-acetyl-5-((3-(3,4-dihydroxyphenyl)acryloyl)oxy)-4-deoxy-2,3-*O*-isopropylidene-4-seleno-D- ribofuranoside (SG-4a) was obtained as oil (83 %). ^{1}H NMR (500 MHz, $CDCl_3$, Fig. S4): δ 7.63 (d, J = 15.9 Hz, 1H, H8), 7.11 (d, J = 1.3 Hz, 1H, H10), 7.05 (dd, J = 8.2, 1.3 Hz, 1H, H14), 6.91 (d, J = 8.1 Hz, 1H, H13), 6.32 (d, J = 15.9 Hz, 1H, H7), 6.29 (bs, 1H, H1), 5.74 (s, 1H, OH), 5.62 (s, 1H, OH), 5.05 (bd, J = 5.4 Hz, 1H, H3), 5.03 (bd, J = 5.4 Hz, 1H, H2), 4.44 (dd, J = 11.6, 5.7 Hz, 1H, H5b), 4.37 (dd, J = 11.3, 10.6 Hz, 1H, H5a), 3.93 (dd, 1H, J = 10.3, 5.7 Hz, H4), 2.11 (s, 3H, CH_3), 1.55 (s, 3H, CH_3), 1.36 (s, 3H, CH_3). ^{13}C NMR (125 MHz, $CDCl_3$, Fig. S4): δ 169.4, 166.9, 146.2, 145.5, 143.7, 127.5, 122.7, 115.6, 115.1, 114.4, 110.8, 90.2, 86.7, 82.6, 66.3, 48.3, 26.6, 24.7, 21.3. Anal. Calcd for $C_{19}H_{22}O_8Se$: C, 49.90; H, 4.85. Found: C, 49.85; H, 4.77.

(*E*)-*O*-acetyl-5-((3-(4-hydroxy-3-methoxyphenyl)acryloyl)oxy)-4-deoxy-2,3-*O*-isopropylidene-4-seleno-D-ribofuranoside (SG-5a) was obtained as a pale yellow-syrup (0.401 g, 0.850 mmol, 85 %). ^{1}H NMR (500 MHz, $CDCl_3$, Fig. S5): δ 7.67 (d, J = 15.9 Hz, 1H, H8), 7.10 (dd, J = 8.2, 1.0 Hz, 1H, H14), 7.05 (d, J = 1.0 Hz, 1H, H10), 6.94 (d, J = 8.1 Hz, 1H, H13), 6.33 (d, J = 15.9 Hz, 1H, H7), 6.30 (bs, 1H, H1), 5.97 (s, 1H, OH), 5.05 (bd, J = 5.4 Hz, 1H, H3), 5.02 (bd, J = 5.4 Hz, 1H, H2), 4.44 (dd, J = 11.6, 5.7 Hz, 1H, H5a), 4.34 (dd, J = 11.3, 10.6 Hz, 1H, H5b), 4.02–3.86 (m, 4H, H4, OCH_3), 2.1 (s, 3H, CH_3), 1.54 (s, 3H, CH_3), 1.35 (s, 3H, CH_3), ^{13}C NMR (125 MHz, $CDCl_3$, Fig. S5): δ 169.3, 166.8, 148.2, 146.8, 145.7, 126.8, 123.3, 114.8, 114.7, 110.8, 109.4, 90.2, 86.7, 82.6, 66.2, 56.0, 48.4, 26.6, 24.7, 21.3. Anal. Calcd for $C_{20}H_{24}O_8Se$: C, 50.96; H, 5.13. Found: C, 50.95; H, 5.23.

4.5. Removal of the O-isopropylidene group to obtain pure compounds SG-3b, SG-4b, and SG-5b

A CH_3COOH/H_2O (8:2, v/v) solution (3.3 mL) was added to SG "a series" compounds (1.0 mmol each), stirring at 80 °C for 2 h. After solvent evaporation under reduced pressure, the organic layer was washed with Et_2O. The crude residue was purified by silica gel column chromatography ($CHCl_3$:MeOH, 19:1 *v/v*) to give compounds **SG-3b**, **SG-4b**, and **SG-5b**.

(*E*)-*O*-acetyl-5-((3-(4-hydroxyphenyl)acryloyl)oxy)-4-deoxy-4-seleno-D- ribofuranoside (SG-3b) was obtained as oil (71 %). ^{1}H NMR (400 MHz, CD_3OD, Fig. S6): δ 7.64 (d, J = 16.0 Hz, 1H, H8), 7.48 (d, J = 8.4 Hz, 1H, H10), 6.83 (d, J = 8.5 Hz,1H, H11), 6.34 (d, J = 16.0 Hz,1H, H7), 5.83 (bs, 1H, H1), 4.36 (m, 1H, H2), 4.29 (dd, J = 11.5, 8.2 Hz, 1H, H5a), 4.17 (dd, J = 8.7, 2.7 Hz, 1H, H3), 3.8 (m, 1H, H4), 2.05 (s, 3H, CH_3). ^{13}C NMR (100 MHz, CD_3OD, Fig. S6): δ 169.0, 167.5, 159.1, 145.5, 129.8, 125.8, 115.4, 114.4, 78.0, 76.5, 73.0, 66.4, 42.0, 19.5. Anal. Calcd for $C_{16}H_{18}O_7Se$: C, 47.89; H, 4.52. Found: C, 47.88; H, 4.61.

(*E*)-*O*-acetyl-5-((3-(3,4-dihydroxyphenyl)acryloyl)oxy)-4-deoxy-4-seleno-D-ribofuranoside (SG-4b) was obtained as oil (69 %). ^{1}H NMR (400 MHz, acetone-d_6, Fig. S7): δ 7.55 (d, J = 15.9 Hz, 1H, H8), 7.17 (d, J = 1.7 Hz, 1H, H10), 7.06 (dd, J = 8.2, 1.7 Hz, 1H, H14), 6.87 (d, J = 8.2 Hz, 1H, H13), 6.28 (d, J = 15.9 Hz, 1H, H7), 5.82 (dd, $J_{H,Se}$ = 13.0 Hz, J = 2.0 Hz, 1H, H1), 4.75 (dd, J = 11.3, 4.9 Hz, 1H, H5b), 4.63 (s, 1H, OH), 4.41 (m, 1H, H2), 4.26 (dd, J = 11.3, 8.1 Hz, 1H, H5a), 4.22 (dd, J = 8.6, 3.2 Hz, 1H, H3), 3.84 (ddd, J = 8.3, 4.9, 3.2 Hz, 1H, H4), 2.02 (s, 3H, CH_3). ^{13}C NMR (100 MHz, acetone-d_6, Fig. S7): δ 169.4, 166.2, 148.0, 145.5, 145.3, 126.7, 121.7, 115.5, 114.4, 114.3, 78.6, 77.0, 75.9, 66.4, 42.5, 20.1. Anal. Calcd for $C_{16}H_{18}O_8Se$: C, 46.06; H, 4.35. Found: C, 46.10; H, 4.31.

(*E*)-*O*-acetyl-5-((3-(4-hydroxy-3-methoxyphenyl)acryloyl)oxy)-4-deoxy-4-seleno-D-ribofuranoside (**SG-5b**) was obtained as an amorphous solid (0.345 g, 0.8 mmol, 80 %). ^{1}H NMR (400 MHz, CD_3OD, Fig. S8): δ 7.61 (d, J = 15.9 Hz, 1H, H8), 7.19 (d, J = 1.7 Hz, 1H, H10), 7.07 (dd, J = 8.2, 1.7 Hz, 1H, H14), 6.80 (d, J = 8.2 Hz, 1H, H13), 6.36 (d, J = 15.9 Hz, 1H, H7), 5.80 (dd, $J_{H,Se}$ = 13.0 Hz, J = 2.0 Hz, 1H, H1), 4.75 (dd, J = 11.3, 4.9 Hz, 1H, H5b), 4.58 (s, 1H, OH), 4.34 (m, 1H, H2), 4.26 (dd, J = 11.3, 8.1 Hz, 1H, H5a), 4.16 (dd, J = 8.6, 3.2 Hz, 1H, H3), 3.98 (s, 3H, CH_3), 3.82 (ddd, J = 8.3, 4.9, 3.2 Hz, 1H, H4), 2.03 (s, 3H, CH_3). ^{13}C NMR (100 MHz, CD_3OD, Fig. S8): δ 170.1, 167.3, 149.3, 148.0, 145.8, 126.2, 122.9, 115.1, 113.6, 110.2, 78.0, 76.5, 75.8, 66.3, 55.0, 41.9, 19.5. Anal. Calcd for $C_{17}H_{20}O_8Se$: C, 47.34; H, 4.67. Found: C, 47.43; H, 4.73.

4.6. Radical scavenging activity

The scavenging capacity of **SG-3b**, **SG-4b**, and **SG-5b** was assessed using two different probes: 2,2-diphenyl-1-picrylhydrazyl (DPPH) and 2,2-azinobis-(3-ethylbenzothiazolin-6-sulfonic) (ABTS). Details about the experimental procedures can be found in Ref. [59]. In both methods, the compound concentrations (final levels) were equal to 5, 12.5, 25, and 50 μM. IC_{50} values were also calculated.

4.7. Cell culture and cytotoxicity assessment

Immortalized human keratinocytes (HaCaT) and neuroblastoma cell line (SH-SY5Y) were cultured in Dulbecco's Modified Eagle's Medium (DMEM) supplemented with 10 % fetal bovine serum, 50.0 U/mL of penicillin and 100.0 μg/mL of streptomycin, at 37 °C in a humidified atmosphere, with 5 % CO_2. Cells were seeded in 96-multiwell plates at a density equal to 1.0×10^4 cells/well, and exposed, after 24 h, to **SG-3b**, **SG-4b** and **SG-5b** (1, 5, 10, 25, 50, 100, and 250 μM, final concentrations). MTT [3-(4,5-dimethylthiazol-2-yl)-2,5-diphenyl tetrazolium bromide] assay was performed 24 h after treatment according to Ref. [33]. IC_{50} values were also calculated.

4.8. Cell response to H_2O_2 insult after co-treatment, pre-treatment, and post-treatment with SG compounds

HaCaT cells were firstly exposed for 1 h to increasing doses of H_2O_2 (0.5–5 mM) to determine the concentration able to inhibit the cell mitochondrial redox activity by 35 %. The protective role of the investigated compounds (**SG-3b**, **SG-4b**, and **SG-5b**) was established in cells pre-treated for 24 h, and then exposed to H_2O_2 insult for 1 h (pre-treatment); or cells treated with the Se-glycoconjugates and concomitantly with H_2O_2 for 1 h (co-treatment); or cells exposed to the H_2O_2 insult for 1 h and then treated with the compounds under study for 24 h (post-treatment). At the end of each protocol, cells were washed twice with phosphate-buffered saline (PBS). Then, cell viability was assessed by MTT assay. The RAI% was compared to cells treated only with H_2O_2 for 1 h, used as the positive control [33].

4.9. Compound cell uptake: UHPLC–HRMS based metabolomics

The cell uptake levels in the human keratinocyte cell line (1.5×10^6 cells in a Petri dish) were estimated as previously described [19] after treatment with **SG-3b**, **SG-4b**, and **SG-5b** (25 μM, final concentration) for 24 h. UHPLC-HRMS analysis was assessed on the samples obtained at the end of the metabolomic protocol. The NEXERA UHPLC system (Shimadzu, Tokyo, Japan) supplied with a Luna® Omega C18 column (1.6 μm particle size, 50 × 2.1 mm i.d., Phenomenex, Torrance, CA, USA) was used for chromatographic analyses. A binary solution consisting of 75 % H_2O and 25 % CH_3CN (both acidified with 0.1 % HCOOH) served as the mobile phase in isocratic conditions, with a flow rate of 0.5 mL/min (5 min run time) and the injection volume of 2 μL. The AB SCIEX Triple TOF® 4600 mass spectrometer was used for compound detection, employing the same parameters previously reported (paragraph 4.1.). For quantitation purposes, the calibration curves were constructed for each analyte in the concentration range of 6.1–50.0 μM.

4.10. In vitro skin permeation analysis

4.10.1. Penetration assay on static vertical diffusion Franz cells

The skin permeation absorption of HCAs (**3**, **4**, and **5**), FG and SG Se-glycoconjugates (both labeled as **3b**, **4b**, and **5b**) was carried out using static vertical diffusion Franz cells (Lara-Spiral, Courtenon, France) [60]. The Institutional Review Board and Animal Ethics Committee of the Universitat Autònoma de Barcelona (Spain) approved the animal handling protocol (reference 12111, June 11, 2024), which complied with the "*Guide for the Care and Use of Laboratory Animals*" of the US National Institutes of Health (Institute of Laboratory Animal Research). The porcine skin was obtained from the unboiled dorsal region of domestic pigs. Following the removal of most subcutaneous fat using a scalpel, the skin was rinsed with tap water and then dermatomed to a thickness of 500 μm ± 50 μm using a Dermatome GA630 (Aesculap, Germany). Subsequently, the skin was cut into appropriate pieces (2.5 cm diameter, 1.86 cm^2 nominal surface area) and stored at 20 °C. Penetration cells (3 mL, 1.86 cm^2, Lara-Spiral, Courtenon, France) comprised upper donor and lower receptor chambers separated by a skin biopsy. The receptor solution, consisting in bovine serum albumin-added phosphate-buffer saline at pH 7.4 (Sigma, St. Louis MO, USA), was prepared. Before placing the skin onto the lower part of the cell with the *stratum corneum* facing the donor chamber, a magnetic stirring bar was introduced. The lower chamber was filled with receptor fluid via the lateral inlet of the cell using a Pasteur pipette (~3 mL). The penetration cells were clamped and placed in a thermostatically controlled water bath (40 °C) equipped with a magnetic stirring device to maintain the skin's surface temperature at 32 ± 1 °C. The integrity of the skin samples was assessed by measuring transepidermal water loss (TEWL) using a Tewameter MDD-TM300 (Courage & Khazaka, Cologne, Germany). Each compound solution (20 μL) in approximately 1 % *w/v* in ethanol:water 75:25 (*v/v*) was applied to the skin surface. Three diffusion cells were employed for the experimental assay, with an additional cell serving as a control. Following a 24-h exposure time, the skin surface (W) was washed with an aqueous solution containing 0.5 % (*w/w*) sodium lauryl ether sulfate (Merck, Darmstadt, Germany) to remove any excess compound. Subsequently, various components of the skin biopsy (*stratum corneum* (SC), viable epidermis (E), dermis (D), receptor fluid (RF), and rest of skin(R)) were recovered, and extracted and/or diluted in methanol, as follows. To determine the FG and SG, or HCA content, RF was directly analyzed, while excess W fluids were each added to 10 mL of solvent; SC tapes were placed in 2 mL of solvent, and viable E, D, and R samples were placed in a volume of 1 mL. All samples were extracted overnight in methanol and filtered through a 0.45 μm Nylon filter (Cameo, Sigma-Aldrich, St. Louis, MO, USA) before HPLC-DAD analysis.

4.10.2. HPLC-DAD quantitative analysis

In order to assess the amount of the compounds absorbed through the skin layer of the Cell Franz diffusion test, quantitative analysis was performed by HPLC-DAD. The extracts (obtained as described in previous section) were analyzed using HPLC (Hitachi Elite LaChrom; Darmstadt, Germany), equipped with an L-2130 Pump, L-2200 Autosampler, and 5430 Diode assay Detector, controlled using EZChrom Elite software v3.1.6. The column was a LiChrosphere 100/Lichrochart 250-5 RP-18 (5 μm) (Darmstadt, Germany). The injection volume was 20 μL. Elution conditions for the detection involved water acidified with 1 % HCOOH (A) and acetonitrile (B) with isocratic elution at 27 % B and a flow rate of 1 mL/min. The detection parameters are detailed in Table 1 (wavelength and retention time) which also includes the calibration curve and linear regression equations ($R^2 > 0.999$) for each analyzed compound. Octanol-water partition coefficients (Log *P*) and molecular

Table 1
HPLC analytical conditions and Molecular weight (MW), molecular volume, and octanol-water partition coefficients (Log *P*) obtained from the Molinspiration platform.

		λ (nm)	t_R (min)	Equation	R^2	Linearity range (μg/mL)	Log *P*	Molecular volume	MW(g/mol)
HCAs	**3**	305	5.57	y = 646660.20x-130773.00	0.9999	107–0.214	1.43	146.48	164.16
	4	325	3.88	y = 330746.34x-350221.00	0.9996	102–0.816	0.94	154.5	180.16
	5	325	5.72	y = 382598.10x-324945.50	0.9995	112–0.448	1.25	194.19	194.18
FG	**3b**	305	8.65	y = 286535.94x-68084.23	0.9999	100–0.200	1.25	260.22	343.24
	4b	325	5.86	y = 110081.50x-64851.50	0.9999	100–0.800	0.76	268.24	359.24
	5b	325	9.64	y = 94107.00x-41955.68	0.9997	100–0.800	1.07	285.76	373.26
SG	**3b**	305	10.53	y = 185307.55x-155304.01	0.9997	100–0.800	1.29	304.77	401.27
	4b	325	7.87	y = 109257.29x-66268.93	0.9998	100–0.800	0.81	312.79	417.27
	5b	325	11.98	y = 174152.42x-138634.08	0.9999	100–0.800	1.11	330.32	431.30

volume were predicted by the Molinspiration model suggesting the skin permeability of compounds [61]. The obtained data were also presented as normalized amounts (%).

4.11. Statistical analysis

Results of anti-radical were based on two independent experiments, each performed in triplicate (in total, 2 × 3 measurements. Cytotoxic effects by MTT and in-cell antioxidant activity were evaluated, based on six replicates from two independent experiments (in total: 2 × 6 measurements). All data were expressed as mean ± standard deviation (SD). $p < 0.05$ values indicated a statistically significant difference.

CRediT authorship contribution statement

Giovanna Cimmino: Writing – original draft, Validation, Investigation, Formal analysis, Data curation. **Mauro De Nisco:** Visualization, Methodology, Investigation, Conceptualization. **Cristina Alonso:** Visualization, Validation, Methodology, Investigation. **Claudia Gravina:** Investigation. **Vincenzo Piscopo:** Visualization, Formal analysis. **Reinier Lemos:** Formal analysis. **Luisa Coderch:** Visualization, Methodology. **Simona Piccolella:** Writing – original draft, Investigation, Data curation. **Severina Pacifico:** Writing – review & editing, Visualization, Supervision, Resources, Methodology, Data curation, Conceptualization. **Silvana Pedatella:** Visualization, Supervision, Resources, Methodology, Conceptualization.

Declaration of competing interest

The authors declare that they have no known competing financial interests or personal relationships that could have appeared to influence the work reported in this paper.

Appendix A. Supplementary data

Supplementary data to this article can be found online at https://doi.org/10.1016/j.ejmcr.2024.100240.

Data availability

Data will be made available on request.

References

[1] E. Alvarez, R. Villa, S. Nieto, A. Donaire, E. García-Verdugo, S.V. Luis, P. Lozano, The suitability of lipases for the synthesis of bioactive compounds with cosmeceutical applications, Mini-Rev, Org. Chem. 18 (2021) 515–528, https://doi.org/10.2174/1570193x17999200805215623.

[2] D.J. Newman, G.M. Cragg, Natural products as sources of new drugs from 1981 to 2014, J. Nat. Prod. 79 (2016) 629–661, https://doi.org/10.1021/acs.jnatprod.5b01055.

[3] A. Fernandes, P.M. Rodrigues, M. Pintado, F.K. Tavaria, A systematic review of natural products for skin applications: Targeting inflammation, wound healing, and photo-aging, Phytomedicine 115 (2023) 154824, https://doi.org/10.1016/j.phymed.2023.154824.

[4] Fortune Business Insights, The global cosmeceuticals market size is projected to grow from $68, 67 billion in 2024 to $138.26 billion by 2032, at a CAGR of 9.1% during the forecast period, Available online: https://www.fortunebusinessinsights.com/cosmeceuticals-market-102521. (Accessed 26 June 2024).

[5] P. Morganti, M.-B. Coltelli, A new carrier for advanced cosmeceuticals, Cosmetics 6 (2019) 10, https://doi.org/10.3390/cosmetics6010010.

[6] P. Morganti, G. Morganti, H.-D. Chen, M.-B. Coltelli, A. Gagliardini, Smart tissue carriers for innovative cosmeceuticals and nutraceuticals, Cosmetics 11 (2024) 20, https://doi.org/10.3390/cosmetics11010020.

[7] C. Oliveira, C. Coelho, J.A. Teixeira, P. Ferreira-Santos, C.M. Botelho, Nanocarriers as active ingredients enhancers in the cosmetic industry—the European and North America regulation challenges, Molecules 27 (2022) 1669, https://doi.org/10.3390/molecules27051669.

[8] J.J. Darrow, J. Avorn, A.S. Kesselheim, FDA approval and regulation of pharmaceuticals, 1983-2018, JAMA 323 (2020) 164, https://doi.org/10.1001/jama.2019.20288.

[9] B. Zegarska, L. Rudnicka, J. Narbutt, W. Barańska-Rybak, B. Bergler-Czop, E. Chlebus, M. Czarnecka-Operacz, J. Czuwara, A. Kaszuba, R. Nowicki, A. Owczarczyk-Saczonek, W. Placek, M. Sokołowska-Wojdyło, J. Szepietowski, Dermo-cosmetics in dermatological practice. Recommendations of the polish dermatological Society. Part I, Dermatol. Rev. 110 (2023) 121–132, https://doi.org/10.5114/dr.2023.127834.

[10] M. Amer, M. Maged, Cosmeceuticals versus pharmaceuticals, Clin. Dermatol. 27 (2009) 428–430, https://doi.org/10.1016/j.clindermatol.2009.05.004.

[11] P. Diao, H. He, J. Tang, L. Xiong, L. Li, Natural compounds protect the skin from airborne particulate matter by attenuating oxidative stress, Biomed. Pharmacother. 138 (2021) 111534, https://doi.org/10.1016/j.biopha.2021.111534.

[12] J. Chen, Y. Liu, Z. Zhao, J. Qiu, Oxidative stress in the skin: impact and related protection, Int. J. Cosmet. Sci. 43 (2021) 495–509, https://doi.org/10.1111/ics.12728.

[13] J.C. Chamcheu, A.L. Walker, F.K. Noubissi, Natural and synthetic bioactives for skin health, disease and management, Nutrients 13 (2021) 4383, https://doi.org/10.3390/nu13124383.

[14] E.C. Milam, A. Price, S. Ramachandran, D.E. Cohen, Contact dermatitis and topical agents, in: Cosmetic Dermatology, Wiley, 2022, pp. 57–71, https://doi.org/10.1002/9781119676881.ch6.

[15] C. Espinosa-Leal, S. Garcia-Lara, Current methods for the discovery of new active ingredients from natural products for cosmeceutical applications, Planta Med. 85 (2019) 535–551, https://doi.org/10.1055/a-0857-6633.

[16] K. Jakubczyk, A. Nowak, A. Muzykiewicz-Szymańska, Ł. Kucharski, K. Szymczykowska, K. Janda-Milczarek, Kombucha as a potential active ingredient in cosmetics—an ex vivo skin permeation study, Molecules 29 (2024) 1018, https://doi.org/10.3390/molecules29051018.

[17] H. Deng, Q. Xu, H.-Y. Guo, X. Huang, F. Chen, L. Jin, Z.-S. Quan, Q.-K. Shen, Application of cinnamic acid in the structural modification of natural products: a review, Phytochemistry 206 (2023) 113532, https://doi.org/10.1016/j.phytochem.2022.113532.

[18] S. Sathyaseelan, B.H. Rao, S. Anushmati, Cosmeceuticals: a transit state from synthetic to natural, Indian J. Pharmacol. 56 (2024) 42–51, https://doi.org/10.4103/ijp.ijp_244_21.

[19] G. Cimmino, M. De Nisco, S. Piccolella, C. Gravina, S. Pedatella, S. Pacifico, Innovative cosmeceutical ingredients: harnessing selenosugar-linked hydroxycinnamic acids for antioxidant and wound-healing properties, Antioxidants 13 (2024) 744, https://doi.org/10.3390/antiox13060744.

[20] H.-Y. Tsai, J.-F. Yang, Y.-B. Chen, J.-L. Guo, S. Li, G.-J. Wei, C.-T. Ho, J.-L. Hsu, C.-I. Chang, Y.-S. Liang, H.-S. Yu, Y.-K. Chen, Acetylation enhances the anticancer

activity and oral bioavailability of 5-demethyltangeretin, Int. J. Mol. Sci. 23 (2022) 13284, https://doi.org/10.3390/ijms232113284.
[21] K. Sakao, H. Saruwatari, S. Minami, D.-X. Hou, Hydroxyl group acetylation of quercetin enhances intracellular absorption and persistence to upregulate anticancer activity in HepG2 cells, Int. J. Mol. Sci. 24 (2023) 16652, https://doi.org/10.3390/ijms242316652.
[22] L. Serpico, M. De Nisco, F. Cermola, M. Manfra, S. Pedatella, Stereoselective synthesis of selenium-containing glycoconjugates via the Mitsunobu reaction, Molecules 26 (2021) 2541, https://doi.org/10.3390/molecules26092541.
[23] N. Veerapen, S.A. Taylor, C.J. Walsby, B.M. Pinto, A mild Pummerer-like reaction of carbohydrate-based selenoethers and thioethers involving linear ozonide acetates as putative intermediates, J. Am. Chem. Soc. 128 (2005) 227–239, https://doi.org/10.1021/ja0557029.
[24] D.P. Demarque, A.E.M. Crotti, R. Vessecchi, J.L.C. Lopes, N.P. Lopes, Fragmentation reactions using electrospray ionization mass spectrometry: an important tool for the structural elucidation and characterization of synthetic and natural products, Nat. Prod. Rep. 33 (2016) 1650–1673, https://doi.org/10.1039/C5NP00073D.
[25] I.G. Munteanu, C. Apetrei, Analytical methods used in determining antioxidant activity: a review, Int. J. Mol. Sci. 22 (2021) 3380, https://doi.org/10.3390/ijms22073380.
[26] W. Lewandowski, H. Lewandowska, A. Golonko, G. Świderski, R. Świsłocka, M. Kalinowska, Correlations between molecular structure and biological activity in "logical series" of dietary chromone derivatives, PLoS One 15 (2020) e0229477, https://doi.org/10.1371/journal.pone.0229477.
[27] N.C. Charlton, M. Mastyugin, B. Török, M. Török, Structural features of small molecule antioxidants and strategic modifications to improve potential bioactivity, Molecules 28 (2023) 1057, https://doi.org/10.3390/molecules28031057.
[28] R. Wołosiak, B. Drużyńska, D. Derewiaka, M. Piecyk, E. Majewska, M. Ciecierska, E. Worobiej, P. Pakosz, Verification of the conditions for determination of antioxidant activity by ABTS and DPPH assays—a practical approach, Molecules 27 (2022) 50, https://doi.org/10.3390/molecules27010050.
[29] O. Hakeem Oladimeji, P. Omoridion Owere, P. Chidera Anthony, Acetylation of cinnamic acid and evaluation of antioxidant activity of the resultant derivative, Int. J. Bioorg. Chem. 6 (2021) 26, https://doi.org/10.11648/j.ijbc.20210602.13.
[30] K.M. Schaich, X. Tian, J. Xie, Hurdles and pitfalls in measuring antioxidant efficacy: a critical evaluation of ABTS, DPPH, and ORAC assays, J. Funct.Foods 14 (2015) 111–125, https://doi.org/10.1016/j.jff.2015.01.043.
[31] F. Gubitosa, D. Fraternale, R. De Bellis, A. Gorassini, L. Benayada, L. Chiarantini, M.C. Albertini, L. Potenza, Cydonia oblonga Mill. pulp callus inhibits oxidative stress and inflammation in injured cells, Antioxidants 12 (2023) 1076, https://doi.org/10.3390/antiox12051076.
[32] S. Warinhomhoun, C. Muangnoi, V. Buranasudja, W. Mekboonsonglarp, P. Rojsitthisak, K. Likhitwitayawuid, B. Sritularak, Antioxidant activities and protective effects of dendropachol, a new bisbibenzyl compound from Dendrobium pachyglossum, on hydrogen peroxide-induced oxidative stress in HaCaT keratinocytes, Antioxidants 10 (2021) 252, https://doi.org/10.3390/antiox10020252.
[33] S. Piccolella, M. Fiorentino, G. Cimmino, A. Esposito, S. Pacifico, Cilentan Cichorium intybus L. organs: UHPLC-QqTOF-MS/MS analysis for new antioxidant scenario, exploitable locally and beyond, Future Foods 9 (2024) 100379, https://doi.org/10.1016/j.fufo.2024.100379.
[34] I.C. Vlachogianni, E. Fragopoulou, I.K. Kostakis, S. Antonopoulou, In vitro assessment of antioxidant activity of tyrosol, resveratrol and their acetylated derivatives, Food Chem. 177 (2015) 165–173, https://doi.org/10.1016/j.foodchem.2014.12.092.
[35] M. Contardi, M. Lenzuni, F. Fiorentini, M. Summa, R. Bertorelli, G. Suarato, A. Athanassiou, Hydroxycinnamic acids and derivatives formulations for skin damages and disorders: a review, Pharmaceutics 13 (2021) 999, https://doi.org/10.3390/pharmaceutics13070999.
[36] R. Hao, M. Li, F. Li, D. Sun-Waterhouse, D. Li, Protective effects of the phenolic compounds from mung bean hull against H2O2-induced skin aging through alleviating oxidative injury and autophagy in HaCaT cells and HSF cells, Sci. Total Environ. 841 (2022) 156669, https://doi.org/10.1016/j.scitotenv.2022.156669.
[37] T. Pluemsamran, T. Onkoksoong, U. Panich, Caffeic acid and ferulic acid inhibit UVA-induced matrix metalloproteinase-1 through regulation of antioxidant defense system in keratinocyte HaCaT cells, Photochem. Photobiol. 88 (2012) 961–968, https://doi.org/10.1111/j.1751-1097.2012.01118.x.
[38] D.K. Maurya, T.P.A. Devasagayam, Antioxidant and prooxidant nature of hydroxycinnamic acid derivatives ferulic and caffeic acids, Food Chem. Toxicol. 48 (2010) 3369–3373, https://doi.org/10.1016/j.fct.2010.09.006.
[39] J.-Y. Choi, H. Kim, Y.-J. Choi, A. Ishihara, K. Back, S.-G. Lee, Cytoprotective activities of hydroxycinnamic acid amides of serotonin against oxidative stress-induced damage in HepG2 and HaCaT cells, Fitoterapia 81 (2010) 1134–1141, https://doi.org/10.1016/j.fitote.2010.07.015.
[40] D. Zhou, X. Weng, A novel butylated caffeic acid derivative protects HaCaT keratinocytes from squalene peroxidation-induced stress, Skin Pharmacol. Physiol. 32 (2019) 307–317, https://doi.org/10.1159/000501731.
[41] J. Garrido, A. Gaspar, E.M. Garrido, R. Miri, M. Tavakkoli, S. Pourali, L. Saso, F. Borges, O. Firuzi, Alkyl esters of hydroxycinnamic acids with improved antioxidant activity and lipophilicity protect PC12 cells against oxidative stress, Biochimie 94 (2012) 961–967, https://doi.org/10.1016/j.biochi.2011.12.015.
[42] M.J. Davies, C.H. Schiesser, 1,4-Anhydro-4-seleno-d-talit (SeTal): a remarkable selenium-containing therapeutic molecule, New J. Chem. 43 (2019) 9759–9765, https://doi.org/10.1039/c9nj02185j.
[43] R. di Vito, M. Acito, C. Fatigoni, C.H. Schiesser, M.J. Davies, F. Mangiavacchi, M. Villarini, C. Santi, M. Moretti, Genotoxicity assessment of 1,4-anhydro-4-seleno-d-talitol (SeTal) in human liver HepG2 and HepaRG cells, Toxicology 499 (2023) 153663, https://doi.org/10.1016/j.tox.2023.153663.
[44] H.H. Ng, C.H. Leo, K. O'Sullivan, S.-A. Alexander, M.J. Davies, C.H. Schiesser, L. J. Parry, 1,4-Anhydro-4-seleno-D-talitol (SeTal) protects endothelial function in the mouse aorta by scavenging superoxide radicals under conditions of acute oxidative stress, Biochem. Pharmacol. 128 (2017) 34–45, https://doi.org/10.1016/j.bcp.2016.12.019.
[45] T. Zacharias, K. Flouda, T.A. Jepps, B. Gammelgaard, C.H. Schiesser, M.J. Davies, Effects of a novel selenium substituted-sugar (1,4-anhydro-4-seleno-d-talitol, SeTal) on human coronary artery cell lines and mouse aortic rings, Biochem. Pharmacol. 173 (2020) 113631, https://doi.org/10.1016/j.bcp.2019.113631.
[46] C. Storkey, D.I. Pattison, J.M. White, C.H. Schiesser, M.J. Davies, Preventing protein oxidation with sugars: scavenging of hypohalous acids by 5-selenopyranose and 4-selenofuranose derivatives, Chem. Res. Toxicol. 25 (2012) 2589–2599, https://doi.org/10.1021/tx3003593.
[47] J. López-García, M. Lehocký, P. Humpolíček, P. Sáha, HaCaT keratinocytes response on antimicrobial atelocollagen substrates: Extent of cytotoxicity, cell viability and proliferation, J. Funct. Biomater. 5 (2014) 43–57, https://doi.org/10.3390/jfb5020043.
[48] S. Lo, E. Leung, B. Fedrizzi, D. Barker, Syntheses of mono-acylated luteolin derivatives, evaluation of their antiproliferative and radical scavenging activities and implications on their oral bioavailability, Sci. Rep. 11 (2021) 92135, https://doi.org/10.1038/s41598-021-92135-w.
[49] J.D. Lambert, S. Sang, J. Hong, S.-J. Kwon, M.-J. Lee, C.-T. Ho, C.S. Yang, Peracetylation as a means of enhancing in vitro bioactivity and bioavailability of epigallocatechin-3-gallate, Drug Metab. Dispos. 34 (2006) 2111–2116, https://doi.org/10.1124/dmd.106.011460.
[50] L. Zhang, Z. Dong, W. Liu, X. Wu, H. He, Y. Lu, W. Wu, J. Qi, Novel pharmaceutical strategies for enhancing skin penetration of biomacromolecules, Pharmaceutics 15 (2022) 877, https://doi.org/10.3390/ph15070877.
[51] Y.C. Boo, p-Coumaric acid as an active ingredient in cosmetics: a review focusing on its antimelanogenic effects, Antioxidants 8 (2019) 275, https://doi.org/10.3390/antiox8080275.
[52] G. Martimestres, J. Mestres, J. Bres, S. Martin, J. Ramos, L. Vian, The "in vitro" percutaneous penetration of three antioxidant compounds, Int. J. Pharm. 331 (2007) 139–144, https://doi.org/10.1016/j.ijpharm.2006.09.020.
[53] C.-F. Lin, Y.-L. Leu, S.A. Al-Suwayeh, M.-C. Ku, T.-L. Hwang, J.-Y. Fang, Anti-inflammatory activity and percutaneous absorption of quercetin and its polymethoxylated compound and glycosides: the relationships to chemical structures, Eur. J. Pharm. Sci. 47 (2012) 857–864, https://doi.org/10.1016/j.ejps.2012.04.024.
[54] M. Turchi, Q. Cai, G. Lian, An evaluation of in-silico methods for predicting solute partition in multiphase complex fluids – a case study of octanol/water partition coefficient, Chem. Eng. Sci. 197 (2019) 150–158, https://doi.org/10.1016/j.ces.2018.12.003.
[55] S.-Y. Chuang, Y.-K. Lin, C.-F. Lin, P.-W. Wang, E.-L. Chen, J.-Y. Fang, Elucidating the skin delivery of aglycone and glycoside flavonoids: how the structures affect cutaneous absorption, Nutrients 9 (2017) 1304, https://doi.org/10.3390/nu9121304.
[56] J.-Y. Fang, T.-H. Huang, C.-F. Hung, Y.-L. Huang, I.A. Aljuffali, W.-C. Liao, C.-F. Lin, Derivatization of honokiol by integrated acetylation and methylation for improved cutaneous delivery and anti-inflammatory potency, Eur. J. Pharm. Sci. 114 (2018) 189–198, https://doi.org/10.1016/j.ejps.2017.12.007.
[57] G.T. Voss, R.L. de Oliveira, M.J. Davies, W.B. Domingues, V.F. Campos, M. P. Soares, C. Luchese, C.H. Schiesser, E.A. Wilhelm, Suppressive effect of 1,4-Anhydro-4-seleno-d-talitol (SeTal) on atopic dermatitis-like skin lesions in mice through regulation of inflammatory mediators, J. Trace Elem. Med. Biol. 67 (2021) 126795, https://doi.org/10.1016/j.jtemb.2021.126795.
[58] G.T. Voss, M.J. Davies, C.H. Schiesser, R.L. de Oliveira, A.B. Nornberg, V.R. Soares, A.M. Barcellos, C. Luchese, A.R. Fajardo, E.A. Wilhelm, Treating atopic-dermatitis-like skin lesions in mice with gelatin-alginate films containing 1,4-Anhydro-4-seleno-d-talitol (SeTal), Int. J. Pharm. 642 (2023) 123174, https://doi.org/10.1016/j.ijpharm.2023.123174.
[59] S. Pacifico, S. Piccolella, S. Galasso, A. Fiorentino, N. Kretschmer, S.P. Pan, R. Bauer, P. Monaco, Influence of harvest season on chemical composition and bioactivity of wild rue plant hydroalcoholic extracts, Food Chem. Toxicol. 90 (2016) 102–111, https://doi.org/10.1016/j.fct.2016.02.009.
[60] C. Gravina, S. Piccolella, C. Alonso, M. Martí, M. Formato, S. Pacifico, L. Coderch, A. Esposito, Encapsulation of Lavandula austroapennina N.G. Passal., Tundis & Upson extracts: focus on leaf and stem enriched liposome for cosmeceutical innovation, Ind. Crops Prod. 213 (2024) 118362, https://doi.org/10.1016/j.indcrop.2024.118362.
[61] Molinspiration Chemoinformatics software, Available online: https://www.molinspiration.com. (Accessed 15 April 2024).